(Received 21 December 2023, Accepted 18 January 2024, Scheduled 3 February 2024)

Study on Anti-Offset Performance of Dynamic Wireless Charging System with Reverse Series Double-Layer Symmetrical Coil for Electric Vehicles

Xiangfei Li[1], Xin Zhou[1], Shentao Zou[2], Yu Cheng[2], Xiaohua Shu[2,*], Xinbo Xiong[1], Ziyue Gan[1], and Zhongqi Li[2,3,*]

[1] *College of Electrical and Information Engineering, Hunan University of Technology, Zhuzhou 412007, China*
[2] *College of Railway Transportation, Hunan University of Technology, Zhuzhou 412007, China*
[3] *College of Electrical and Information Engineering, Hunan University, Changsha 410082, China*

ABSTRACT: In dynamic wireless charging systems for electric vehicles (EVs), the coupling mechanism is difficult to align, which leads to high output voltage fluctuations and low transmission efficiency of the system. A reverse series double-layer symmetrical coil (RSDSC) structure with magnetic core is proposed. First, the mutual inductance characteristics of this structure are analyzed based on its coupling structure. Secondly, a mutual inductance optimization method is proposed to obtain the optimal values of each parameter of the coil and the optimal values of the magnetic core parameters. Finally, a wireless power transfer system is built based on the obtained coil and magnetic core parameters, and the correctness of the structure is verified through simulation and experimentation. The results show that the maximum mutual inductance fluctuation of the structure of RSDSC with magnetic core is only 4.88%, and the efficiency is up to 97.86% when the receiving coil is offset within 50% (20.8 cm) of the outer length of the transmitting coil.

1. INTRODUCTION

In recent years, wireless power transfer has abandoned the traditional plug-and-play charging method, and at the same time has the advantages of safety, reliability, and aesthetics [1–4]. It makes more and more scholars pay attention and research [5]. Wireless energy transmission technology has a wide range of applications in electric vehicles (EVs), consumer electronics, aerospace, and biomedical fields [6–8]. In the field of EV, the technology can solve the problems of poor range and slow charging speed caused by the existence of insufficient capacity of EV batteries [9–11]. It is favourable to promote the long-term development of new energy EV. In the dynamic wireless charging process of EV, the offset between the transmitting and receiving coils is bound to occur, so the mutual inductance changes, and if it is not improved, the stability of its system will be greatly affected [12–14]. The innovation and optimization of the coil structure can fundamentally improve the stability of the system, so it is of great significance to study a coil structure with excellent anti-offset performance.

In a wireless power transfer system, the traditional single coil structure is difficult to maintain the magnetic flux unchanged during offset, so many scholars began to make structural innovations, combinations, etc. for the coils. A multi-coil structure can make the spatial magnetic field to be superimposed while increasing the area of the coupling structure. When an offset occurs in a multi-coil structure, the mutual inductance between the coils increases and decreases to reach a dynamic equilibrium state, which improves the anti-offset performance of the system. The team at the University of Auckland, New Zealand, proposed a rectangular planar coil structure with an anti-series double D (DD). The structure has some anti-offset properties along with an improved coupling coefficient [15]. The reverse current in the DD structure creates a region of zero magnetic field during the offset. For this reason, the University of Auckland also proposed to orthogonalize a Q-type coil in the middle of a DD-type coil to form a DDQ-type to address the shortcomings of the DD coil, but at the expense of cost [16]. To keep costs down, the team also improved the DDQ into a Bipolar Pad (BPP) coil structure with partially overlapping DD coils. However, both the DDQ and BP structures have better anti-offset performance only in one direction [17]. Thus, the team continued to improve the BP coil structure and proposed a TP coil resembling a Taichi-type coil that forms a mutually decoupled coil. The advantage of the TP coil is that it can realize better anti-offset performance during rotation [18]. In [19], a coil structure is proposed by adding a reverse series coil in the middle of the DD coil, which results in a very low mutual inductance fluctuation rate during the Y-axis excursion. A QD coil structure was proposed in [20]. Although it has a better anti-offset performance in multiple directions, its magnetic field cancellation at the center of the coil leads to a lower coupling strength. Ref. [21] proposed a QDS coil structure by adding a rectangular coil at the center of a QD coil. QDS coils make up for the shortcomings of QD coils and improve offset resistance. A DLDD coil structure was proposed in [22]. Although it has some anti-offset performance, its mutual inductance fluctuation rate is large. In [23], a structure with a

* Corresponding authors: Xiaohua Shu (501185754@qq.com), Zhongqi Li (my3eee@126.com).

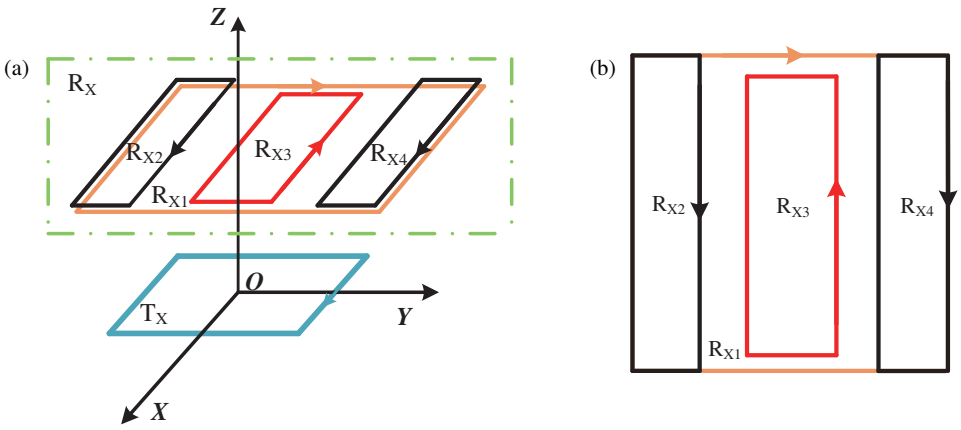

FIGURE 1. Schematic diagram of structure of RSDSC. (a) Structure of RSDSC. (b) Top view of structure of RSDSC.

third coil was proposed by Chen et al. Although it can improve the alignment performance in X and Y directions, its mutual inductance fluctuation rate is 6.4% at 44.4% of the offset transmitter coil diameter. Therefore, it remains a problem to offset a large enough distance in the X-direction and Y-direction and still keep the mutual inductance essentially unchanged when an electric vehicle i charged wirelessly. It has been the research focus of many scholars.

For this reason, a structure with reverse series double-layer symmetrical coil (RSDSC) is proposed in this paper. It not only exhibits high resistance to offset in the direction of motion of the EV but also meets international standards for door side offset distance. The receiving coil of this structure consists of four coils connected in series, with an intermediate coil in reverse series. The mutual inductance between the small coils in the transmitting and receiving coils changes continuously when the coil is offset, but the overall mutual inductance of the transmitting and receiving coils remains essentially unchanged. In addition, a mutual inductance optimization method is proposed to obtain better coil parameters by setting constraints. Meanwhile, based on the optimal coil parameters, a mesh core structure is found to satisfy the requirement of the low fluctuation rate. Finally, the advantages of the proposed structure and the correctness of the optimization method are verified by simulation and experiment. The results show that a 50% offset of the outer length of the transmitting coil can be realized under the direction of motion of an EV, and the mutual sense of the system remains essentially unchanged.

2. STRUCTURE OF RSDSC

In this section, the structure of the RSDSC is analyzed according to the calculation method of mutual inductance [24], and its mutual inductance change rule is derived. The constraints are set according to its changing law, and the mutual inductance is optimized by adjusting the coil parameters to obtain a set of optimal parameters of the coil that satisfy the low fluctuation rate. The magnetic core structure was optimized based on the optimization of the best coil parameters and by setting the initial constraints of the magnetic core. Finally, a set of magnetic core structure parameters that satisfy the low mutual inductance fluctuation rate is obtained.

2.1. Mutual Inductance Characteristics of RSDSC

The structure of RSDSC is shown in Fig. 1. The structure of the RSDSC is composed of a transmitting coil T_X and a receiving coil R_X, both of which are square coils at the periphery. In the receiving coil, R_{X1}, R_{X2}, and R_{X4} are connected in series in the forward direction, and R_{X3} is connected in series in the reverse direction. Meanwhile, the receiving coil of this structure is divided into two layers, R_{X2} and R_{X4} as one layer and R_{X1} and R_{X3} as one layer. The receiver coil is a symmetrical structure. R_{X2} and R_{X4} have identical sizes and are symmetrical about the X-axis. T_X, R_{X1}, and R_{X3} are symmetric about the center of the origin.

The structure of RSDSC has the following two significant features compared to traditional coil structures. Firstly, the receiving coil consists of four coils, with the center coil in reverse series and two coils placed symmetrically on either side. When the coils are offset, the mutual inductance between the transmitting coil and each small coil in the receiving coil changes, but the overall mutual inductance change is small. Secondly, the transmitting coil is slightly smaller than the receiving coil size to reduce the mutual inductance fluctuation rate. The mutual inductance between the transmitting and receiving coils is calculated for the structure of RSDSC according to Newman's formula:

$$M_{Tx-Rx} = M_{Tx-Rx1} + M_{Tx-Rx2} - M_{Tx-Rx3} + M_{Tx-Rx4} \quad (1)$$

where $M_{\mathrm{Tx-Rx-1}}$, $M_{\mathrm{Tx-Rx-2}}$, $M_{\mathrm{Tx-Rx-3}}$, and $M_{\mathrm{Tx-Rx-4}}$ represent the mutual inductance between T_X and R_{X1}, R_{X2}, R_{X3}, and R_{X4}, respectively.

According to the structural characteristics of this coil and the mutual inductance calculation formula [24], the following law can be derived from the analysis. When the receiving coil is offset in the direction of the Y-axis, the mutual inductance of $M_{\mathrm{Tx-Rx-1}}$ and $M_{\mathrm{Tx-Rx-2}}$ decreases, while the mutual inductance of $M_{\mathrm{Tx-Rx-3}}$ and $M_{\mathrm{Tx-Rx-4}}$ increases. Therefore, the mutual inductance values $M_{\mathrm{Tx-Rx}}$ in the Y-direction can be

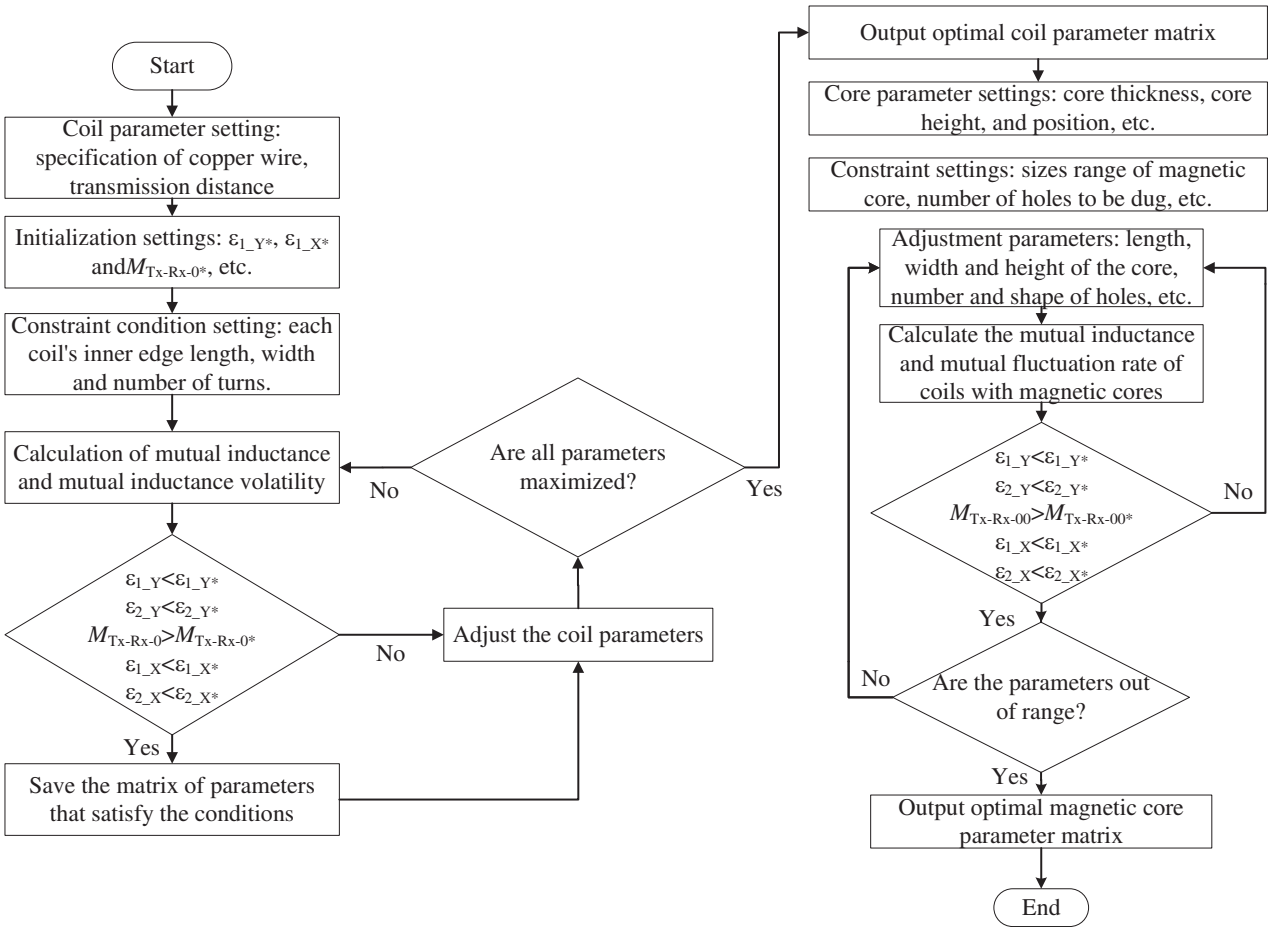

FIGURE 2. Flowchart of mutual inductance optimization method.

guaranteed to achieve quasi-constant by simply ensuring that $M_{\text{Tx}-\text{Rx}-1}$ and $M_{\text{Tx}-\text{Rx}-2}$ decrease by an amount equal to the increase in $M_{\text{Tx}-\text{Rx}-3}$ and $M_{\text{Tx}-\text{Rx}-4}$. When the receiving coil is offset in the direction of the X-axis, the mutual inductance of $M_{\text{Tx}-\text{Rx}-1}$, $M_{\text{Tx}-\text{Rx}-2}$, and $M_{\text{Tx}-\text{Rx}-4}$ decreases, while the mutual inductance of $M_{\text{Tx}-\text{Rx}-3}$ increases. Similarly, the mutual inductance values $M_{\text{Tx}-\text{Rx}}$ in the X-direction can be guaranteed to achieve quasi-constancy by simply ensuring that $M_{\text{Tx}-\text{Rx}-1}$, $M_{\text{Tx}-\text{Rx}-2}$, and $M_{\text{Tx}-\text{Rx}-4}$ decrease by an amount equal to the increase in $M_{\text{Tx}-\text{Rx}-3}$.

2.2. Mutual Inductance Characteristics of RSDS Coils

In this subsection, the parameters of the structure of the RSDSC are optimized according to the rectangular coil mutual inductance calculation formula [24]. It includes coil parameter optimization and core optimization to achieve the goal of essentially constant mutual inductance. The flowchart for mutual inductance optimization is shown in Fig. 2.

The structure of the RSDSC mutual inductance optimization consists of two main steps. Firstly, the coil parameters are optimized to find the optimal coil parameters. Secondly, magnetic core optimization is carried out on the basis of optimal coil parameters to obtain better results. The specific mutual inductance optimization is divided into the following steps.

(1) Coil parameter setting and initialization: The diameter of the copper wire is set to 3.4 mm. The transmission distance between the transmitter coil and receiver coil is set to 15 cm. $\varepsilon_{1\text{Y}}{}^*$, $\varepsilon_{2\text{Y}}{}^*$, $\varepsilon_{1\text{X}}{}^*$ and $\varepsilon_{2\text{X}}{}^*$ are set to 5%. $M_{\text{Tx}-\text{Rx}-0}{}^*$ is set to 64 μH ($M_{\text{Tx}-\text{Rx}-0}$ is the mutual inductance between T_X and R_X at $\Delta X = 0$ cm and $\Delta Y = 0$ cm, where ΔX and ΔY denote the offset distances along the X-axis and Y-axis directions, respectively). Equation (2) is the mutual inductance fluctuation rate along the Y-axis and X-axis directions. When the Y-axis is offset within half the distance of the outer length of the transmitting coil, $M_{\text{Tx}-\text{Rx}-\text{max}-\text{Y}}$ and $M_{\text{Tx}-\text{Rx}-\text{min}-\text{Y}}$ are the maximum and minimum mutual inductances between T_X and R_X, respectively. $M_{\text{Tx}-\text{Rx}-\text{max}-\text{X}}$ and $M_{\text{Tx}-\text{Rx}-\text{min}-\text{X}}$ are the maximum and minimum mutual inductances between T_X and R_X within 10 cm offset from the X-axis, respectively.

$$\begin{cases} \varepsilon_{1\text{Y}} = (M_{\text{Tx}-\text{Rx}-\text{max}-\text{Y}} - M_{\text{Tx}-\text{Rx}-0})/M_{\text{Tx}-\text{Rx}-0} \\ \varepsilon_{2\text{Y}} = (M_{\text{Tx}-\text{Rx}-\text{min}-\text{Y}} - M_{\text{Tx}-\text{Rx}-0})/M_{\text{Tx}-\text{Rx}-0} \\ \varepsilon_{1\text{X}} = (M_{\text{Tx}-\text{Rx}-\text{max}-\text{X}} - M_{\text{Tx}-\text{Rx}-0})/M_{\text{Tx}-\text{Rx}-0} \\ \varepsilon_{2\text{X}} = (M_{\text{Tx}-\text{Rx}-\text{min}-\text{X}} - M_{\text{Tx}-\text{Rx}-0})/M_{\text{Tx}-\text{Rx}-0} \end{cases} \tag{2}$$

(2) Setting coil constraints: The relevant constraints are set according to the desired requirements. In this structure, the inner edge length $l_{1-\text{inner}}$ of $\text{R}_{\text{X}1}$ ranges from 52 to 56 cm. $\text{R}_{\text{X}2}$ inner edge length $l_{2-\text{inner}}$ ranges from 14 to 18 cm. Its inner edge width $W_{2-\text{inner}}$ ranges from 58 to 60 cm. The $\text{R}_{\text{X}3}$ inner edge

TABLE 1. The parameters of RSDSC.

Coils	Inner length/cm	Inner width/cm	Outside length/cm	Outside width/cm	Turns
T_x	28	28	41.6	41.6	20
R_{x1}	54	54	67.6	67.6	20
R_{x2}	16	60	23.5	67.5	11
R_{x3}	17	46	21.8	50.8	6
R_{x4}	16	60	23.5	67.5	11

length $l_{3-\text{inner}}$ ranges from 14 to 18 cm, Its inner edge width $W_{3-\text{inner}}$ ranges from 44 to 48 cm. The inner edge length $l_{4-\text{inner}}$ of T_X ranges from 28 to 30 cm. The number of turns N_1 of R_{X1} is 18 to 24. The number of turns N_2 of R_{X2} is 8 to 14. The number of turns N_3 of R_{X3} ranges from 4 to 8. The number of turns N_4 of T_X is 18 to 22. The step size for the number of turns is 1 turn, and the step size for the side lengths is all 1 cm. The smaller the step of the edge length is, the more data is in Matlab that meets the requirements.

(3) Mutual inductance of coil calculation: According to the mutual inductance formula [24], the mutual inductance between T_X and R_X at coil offset can be calculated. According to Equation (2), ε_{1Y}, ε_{2Y}, ε_{1X}, and ε_{2X} can be calculated.

(4) Conditional judgment: In order to obtain the desired coil parameters, the conditions $\varepsilon_{1Y}<\varepsilon_{1Y}^*$, $\varepsilon_{2Y}<\varepsilon_{2Y}^*$, $\varepsilon_{1X}<\varepsilon_{1X}^*$, $\varepsilon_{2X}<\varepsilon_{2X}^*$, and $M_{\text{Tx}-\text{Rx}-0}>M_{\text{Tx}-\text{Rx}-0}^*$ must be satisfied. If the above conditions are met, the result is saved. If the parameters of coils reach their maximum values, the optimization procedure of coil mutual inductance is terminated. Otherwise, the parameters of the coil continue to be changed.

(5) Output compliant data: The results of the optimal coil parameter matrix are saved and output.

(6) Magnetic core parameter setting: The magnetic core parameters are set on the basis of the optimal coil parameters. The magnetic core is divided into two pieces, the magnetic core of transmitter coil and the magnetic core of receiver coil. The magnetic core of transmitter coil is placed below the transmitting coil, and the magnetic core of receiving coil is placed above the receiving coil. The core thickness is set to 10 mm. $M_{\text{Tx}-\text{Rx}-00}^*$ is set to 98 μH ($M_{\text{Tx}-\text{Rx}-00}$ is the mutual inductance between T_X and R_X at $\Delta X = 0$ cm and $\Delta Y = 0$ cm with magnetic core).

(7) Setting magnetic core constraints: The structure of magnetic core is designed according to the optimized coil mechanism dimensions. The outermost edge length of the structure of magnetic core is set so that both its length and width are smaller than the outermost length and width of the coil. The magnetic cores of the transmitting and receiving coils are processed by digging holes respectively. The number of their holes is greater than or equal to 0, while the length and width of their holes are processed according to the coil structure.

(8) Measurement of mutual inductance of coils with magnetic cores: The mutual inductance between T_X and R_X can be measured by ANSYS Maxwell simulation software. The mutual inductance fluctuation rate ε_{1Y}, ε_{2Y}, ε_{1X}, and ε_{2X} with magnetic core is calculated using Eq. (2).

(9) Judgment conditions for magnetic cores: In order to obtain the desired parameters of the magnetic core, the conditions $\varepsilon_{1Y}<\varepsilon_{1Y}^*$, $\varepsilon_{2Y}<\varepsilon_{2Y}^*$, $\varepsilon_{1X}<\varepsilon_{1X}^*$, $\varepsilon_{2X}<\varepsilon_{2X}^*$ and $M_{\text{Tx}-\text{Rx}-00}>M_{\text{Tx}-\text{Rx}-00}^*$ must be satisfied. If the result satisfies all the setup conditions, the result is saved. If all parameters of the magnetic core reach their maximum values, the optimization procedure of the magnetic core is terminated. Otherwise, the parameters of the magnetic core continue to be changed.

(10) Derive optimization results: The results of the optimal matrix of magnetic core parameters are saved and output.

2.3. Results of Mutual Inductance Optimization of the RSDSC Structure

2.3.1. Results of RSDSC Optimization

First, the data are filtered using the above optimization process through Matlab software. Secondly, the data that meet the requirements are saved. Finally, the optimal parameters of the data are selected, and optimal parameters are shown in Table 1.

2.3.2. Results of Optimization of Magnetic Core for RSDSC

According to the results of the parameters of the coil derived from coil optimization, further optimization of magnetic core structure is carried out using ANSYS Maxwell software. The results of core optimization show that mesh core can be better close to the mutual inductance change rule between the coils when the magnetic core is not added, and can reduce the core consumables. So the mesh core is chosen. The presence of the reverse series coil presents the weakening of the magnetic field. Therefore, the magnetic core should be kept at a distance from the reverse series coil to improve the coupling coefficient between the transmitting and receiving coils.

The dimensions of the optimized magnetic core are shown in Fig. 3. Below the transmitting coil there is a square skeletonized core with a side length of 41.6 cm, whose outer edges are aligned with the transmitting coil. The magnetic core of the receiving coil is a mesh core. The outermost part of the mesh shape magnetic core is a square with a side length of 67.6 cm. The rectangular magnetic core is symmetrically hollowed out on the left and right sides. The magnetic core above the coils in the reverse series is also skeletonized. The mesh core structure saves about 49.81% of core material compared to that when the core is completely spread over the transmitter and receiver coils.

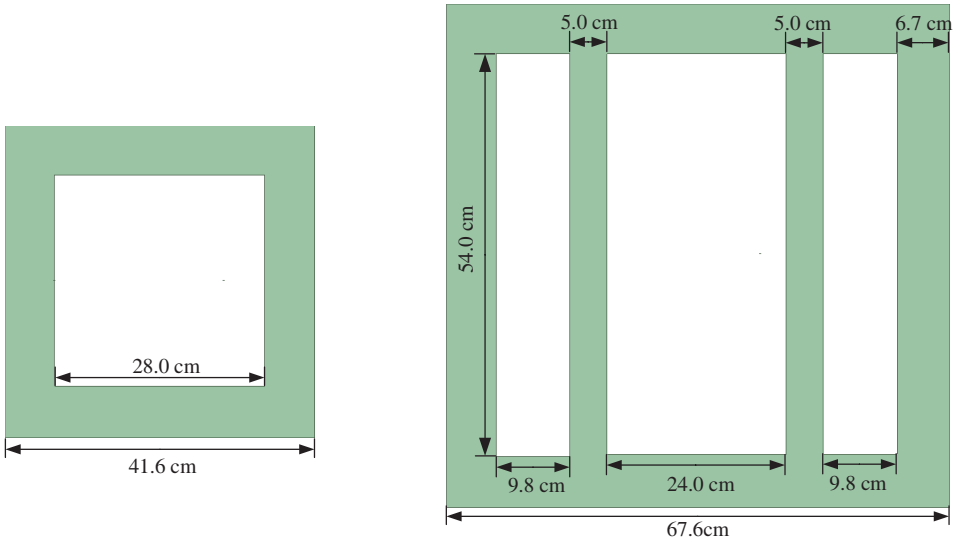

FIGURE 3. Schematic diagram of structure size of magnetic core.

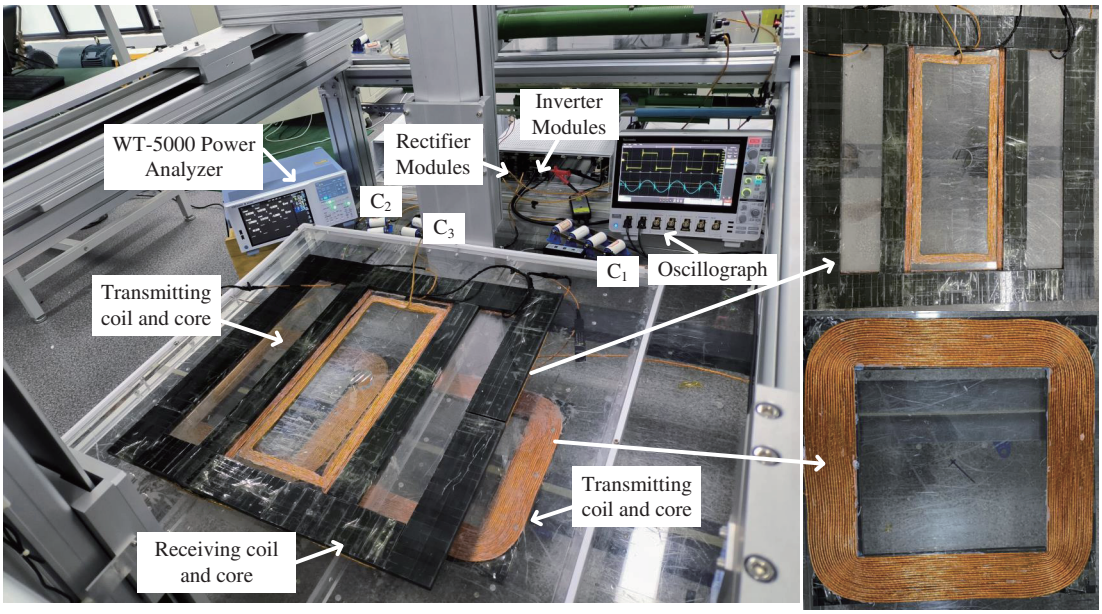

FIGURE 4. Overall experimental diagram.

3. EXPERIMENTAL VALIDATION

3.1. Experimental Setup

Based on the data of the quasi-constant mutual inductance optimization, a physical model conforming to the RSDSC structure is constructed. The specification of the Leeds wire of the coil used is ϕ 0.1 mm $\times$ 600 strands. The experimental model of the rear coil with magnetic core is shown in Fig. 4. Its overall experimental setup includes a DC source, a high-frequency inverter circuit, a transmission coil, a magnetic core, a resonant capacitor, a rectifier circuit, etc. The inverter and rectifier links are silicon carbide power devices, and the model of MOSFET is C3M0075120D. The experimental circuit uses an S-S topology. The frequency of resonant is 85000 Hz.

The IM3536 impedance analyzer is used for self and mutual inductance measurements. The acrylic sheet is used as a frame for coil winding. The data are measured on a wooden table. The final measurements are shown in Table 2.

First, according to the mutual inductance calculation method [24], the mutual inductance is calculated as M_c using Matlab software. Secondly, the simulation is carried out by Ansys Maxwell software to obtain the mutual inductance simulation value M_s. Fig. 5 shows the model of the simulation. Finally, the mutual inductance M_e is measured by the HIOKI IM3536 impedance analyzer. The error between the measured and simulated and calculated values of the mutual inductance is defined as ε_s and ε_e, respectively. The expressions for both

TABLE 2. Parameter measured for coils and coils with magnetic cores.

Parameter	Physical meaning	Value
L_1	Self-inductance of transmitting coil	268.06 μH
$L_1{}^*$	Self-inductance of transmitting coil with magnetic core	383.77 μH
L_2	Self-inductance of receiving coil	1219.16 μH
$L_2{}^*$	Self-inductance of receiving coil with magnetic core	1714.75 μH
C_1	Compensation capacitance of transmitting coil	13.49 nF
$C_1{}^*$	Compensation capacitors with magnetic core transmitting coil	9.04nF
C_2	Compensation capacitance of receiving coil	2.97 nF
$C_2{}^*$	Compensation capacitor with magnetic core receiving coil	1.95 nF
R_1	Parasitic resistance of the transmitting coil	0.186 Ω
$R_1{}^*$	Parasitic resistance of transmitting coil with magnetic core	0.267 Ω
R_2	Parasitic resistance of the receiving coil	0.93 Ω
$R_2{}^*$	Parasitic resistance of receiving coil with magnetic core	1.419 Ω
f_0	Working frequency	85000 Hz

TABLE 3. Calculated, simulated, measured and error rates of mutual inductance along the positive direction of Y-axis.

Misalignment/mm	M_c	M_s	M_e	ε_s/%	ε_e/%
0	66.92	67.12	67.62	0.74	1.04
20.8	67.18	67.26	67.72	0.68	0.95
41.6	67.52	67.68	67.92	0.35	0.59
62.4	68.14	68.29	68.50	0.31	0.53
83.2	68.81	68.95	69.13	0.26	0.46
104	69.32	69.47	69.81	0.49	0.70
124.8	69.49	69.65	70.17	0.74	0.97
145.6	69.15	69.33	69.98	0.93	1.19
166.4	68.18	68.38	69.13	1.09	1.37
187.2	66.54	66.77	67.51	1.10	1.44
208	64.19	64.45	65.28	1.27	1.67

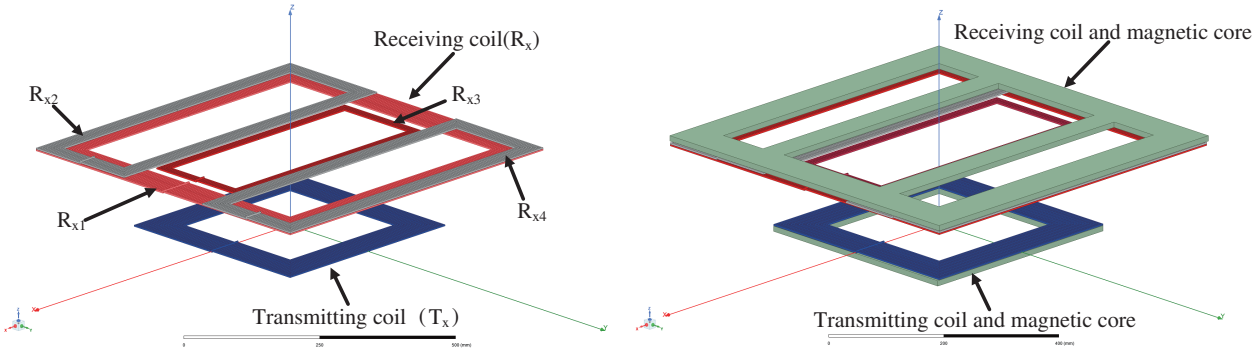

FIGURE 5. Simulation model.

are as follows.

$$\varepsilon_s = \frac{|M_c - M_s|}{M_s} \times 100 \tag{3}$$

$$\varepsilon_e = \frac{|M_c - M_e|}{M_e} \times 100 \tag{4}$$

3.2. Mutual Inductance Verification

3.2.1. Mutual Inductance Verification of RSDSC without Magnetic Cores

From Table 3, it is easy to find that the maximum errors ε_e and ε_s are 1.67% and 1.27%, respectively. The maximum value of mutual inductance is equal to 70.17 μH when the offset distance is 124.8 mm. The minimum value of mutual inductance is equal to 65.28 μH when the offset distance is 208 mm. When the off-

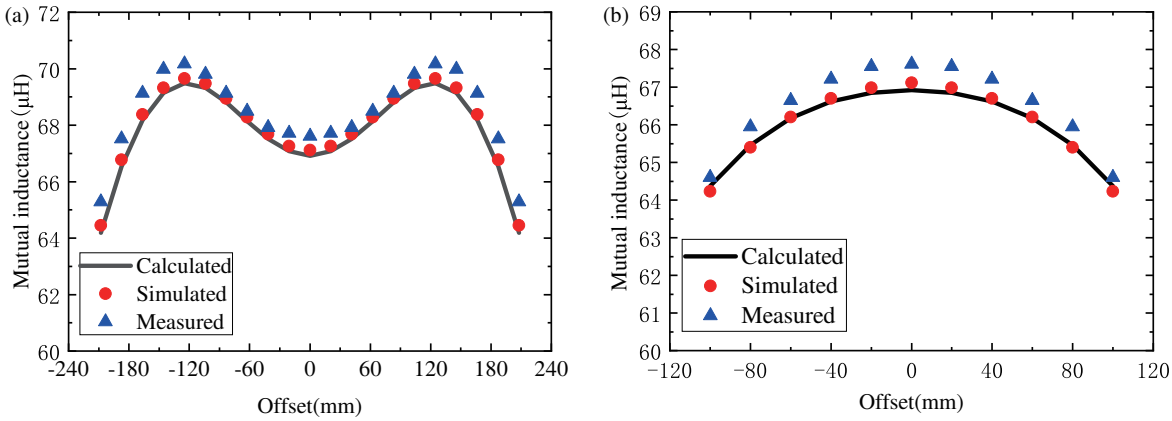

FIGURE 6. Calculated, simulated, and measured values of mutual inductance of RSDSC.

TABLE 4. Calculated, simulated, measured and error rates of mutual inductance along the positive direction of X-axis.

Misalignment/mm	M_c	M_s	M_e	ε_s/%	ε_e/%
0	66.92	67.12	67.62	0.73	1.04
20	66.85	66.98	67.55	0.84	1.04
40	66.62	66.70	67.21	0.76	0.88
60	66.18	66.20	66.65	0.68	0.71
80	65.46	65.41	65.95	0.82	0.74
100	64.37	64.23	64.60	0.57	0.36

set distance is 0 mm, the mutual inductance value is equal to 67.62 μH. According to Eq. (2), the mutual inductance fluctuation rates $\varepsilon_{1Y} = 3.77\%$ and $\varepsilon_{2Y} = 3.46\%$ can be calculated. According to Table 3, the curve of mutual inductance with offset distance in the Y-axis direction was obtained, as shown in Fig. 6(a). The middle point is low, and the ends are high, which is very different from the monotonically decreasing mutual inductance value of the conventional coil structure as the offset distance increases.

From Table 4, it is easy to find that the maximum errors ε_e and ε_s are 1.04% and 0.84%, respectively. The minimum value of mutual inductance is 64.60 μH when the offset is 100 mm. According to Eq. (2), the mutual susceptibility volatility $\varepsilon_{2X} = 4.47\%$ can be calculated. According to Table 3, the curve of X-direction mutual inductance with offset distance is obtained, as shown in Fig. 6(b). From Fig. 6, it is not difficult to find that the X-direction mutual inductance has been decreasing with the increase of the offset distance, which is completely different from the change rule of mutual inductance when it is along the Y-direction.

The results show that the error rates ε_e and ε_s of the structure of the RSDSC are extremely small, verifying the correctness of the mutual inductance optimization of the structure of RSDSC. Meanwhile, it is easy to find from the change curve that the mutual inductance value basically does not change with the change of offset distance, which achieves the goal of quasi-constant mutual inductance.

3.2.2. Mutual Inductance Verification of RSDSC with Magnetic Cores

From Table 5, the maximum error rate ε_s is 2.16%. The maximum value of mutual inductance is 108.42 μH when the offset distance is 124.8 mm. The minimum value of mutual inductance is equal to 99.23 μH when the offset distance is 208 mm. When the offset distance is 0 mm, the mutual inductance value is equal to 103.38 μH. According to Eq. (2), the mutual inductance fluctuation rates $\varepsilon_{1Y} = 4.88\%$ and $\varepsilon_{2Y} = 4.01\%$ can be calculated.

From Table 6, the maximum error rate ε_s is 4.86%. The minimum value of mutual inductance is 98.49 μH when being offset by 100 mm. According to Eq. (2), the mutual inductance fluctuation rate $\varepsilon_{2X} = 4.73\%$ can be calculated.

In order to facilitate the observation of the mutual inductance variation trend of the RSDS coils with magnetic cores, the mutual inductance variation curves with offset distance are obtained according to Tables 5 and 6, as shown in Fig. 7. The results show that the mutual inductance error rate between the simulated and measured values is extremely small, which verifies the correctness of the mutual inductance optimization method for magnetic cores. Meanwhile, it is not difficult to find out from the graph that the RSDSC structure achieves quasi-constant mutual inductance with the mesh core. From Figs. 6 and 7, it can be found that the mutual inductance variation rule with distance is the same for the structure of RSDSC with the magnetic core and the structure of the RSDSC without the magnetic core.

TABLE 5. Simulated values, measured values and error rate along the positive direction of Y-axis.

Misalignment/mm	M_s	M_e	ε_s/%
0	105.46	103.38	2.01
20.8	105.77	103.64	2.06
41.6	106.60	104.43	2.08
62.4	107.76	105.48	2.16
83.2	109.14	106.88	2.11
104	110.11	107.83	2.11
124.8	110.46	108.42	1.88
145.6	109.84	107.64	2.04
166.4	107.96	106.20	1.66
187.2	104.93	103.67	1.22
208	100.44	99.23	1.22

TABLE 6. Simulated values, measured values and error rate along the positive direction of X-axis.

Misalignment/mm	M_s	M_e	ε_s/%
0	105.46	103.38	2.01
20	105.45	102.96	2.41
40	104.92	102.31	2.55
60	103.99	101.67	2.28
80	102.45	100.85	1.58
100	100.03	98.49	1.57

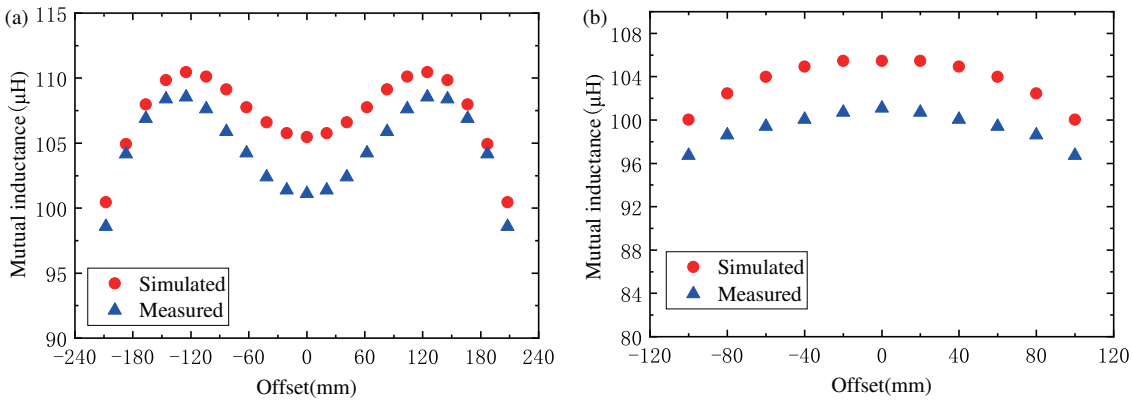

FIGURE 7. Simulated and measured values of mutual inductance for structure of RSDSC with magnetic core. (a) Y-direction. (b) X-direction.

3.3. Tests of Output Power and Transmission Efficiency

A wireless power transfer system was built in order to further test the output power and efficiency of the structure of RSDSC at different offset distances. The experimental setup is shown in Fig. 4. The Yokogawa WT5000 Power Analyzer measures system transfer efficiency to verify the superiority of the structure of RSDSC.

From Fig. 8, the transmission efficiency and output power are 95.08% and 331.25 W when the offset distance is 0 mm, respectively. When the offset distance was within 208 mm, the measured maximum and minimum transmission efficiencies are 97.29% and 94.13%, respectively. The maximum and minimum output powers are 350.74 W and 304.43 W, respectively. The maximum fluctuation rates in transmission efficiency and output power are 2.21% and 8.10%, respectively. As the offset distance increases, the efficiency shows a tendency to increase and then decrease. This is consistent with the trend of mutual sensory changes exhibited in Fig. 6(a).

From Fig. 8(b), the measured maximum and minimum transmission efficiencies are 95.08% and 93.98% when the offset distance along the X-axis is within 100 mm, respectively. The maximum output power is 352.72 W. The maximum fluctuation rates in transmission efficiency and output power are 1.1% and 6.48%, respectively. As the offset distance increases, the efficiency shows a trend of decreasing all the time. This is con-

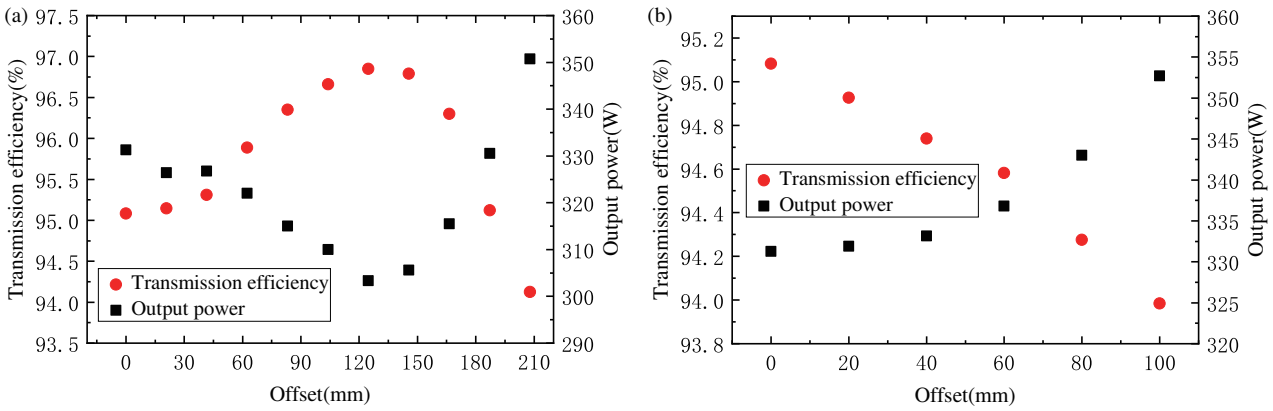

FIGURE 8. Experimental results of output power and transfer efficiency of the structure of RSDSC. (a) Y-direction. (b) X-direction.

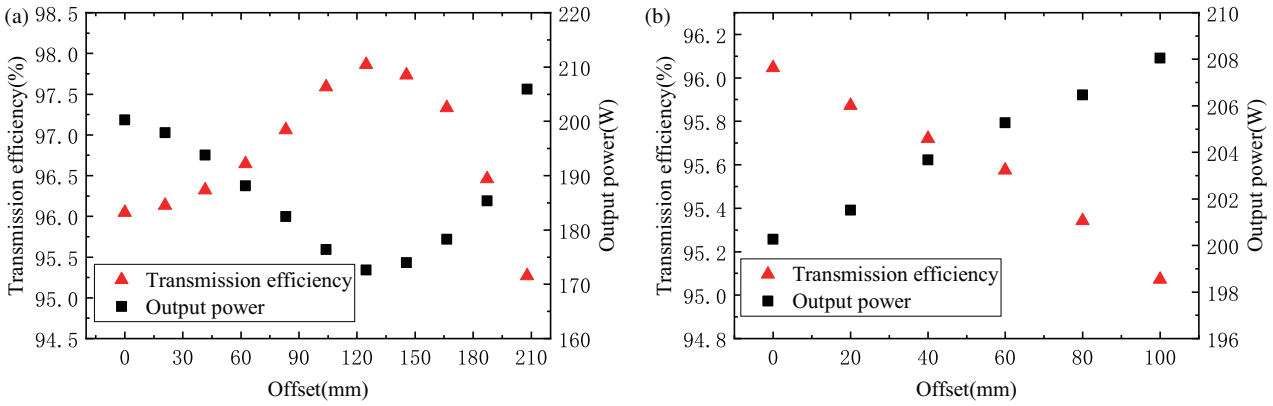

FIGURE 9. Experimental results of output power and transfer efficiency of the structure of RSDSC with magnetic core. (a) Y-direction. (b) X-direction.

sistent with the trend of mutual sensory changes exhibited in Fig. 6(b).

The results show that the fluctuation rate of the transmission efficiency is very small for both offsets to the Y and X direction. The results show that the structure of RSDSC has a very small fluctuation rate of transmission efficiency during the offset process. It is because the mutual inductance is almost constant in this structure, regardless of whether the coil is offset along the Y or X direction.

3.3.1. Structure of RSDSC with Magnetic Core

From Fig. 9(a), the transmission efficiency and output power are 96.06% and 200.27 W, respectively, when the offset distance is 0 cm, respectively. When the offset distance is within 208 mm, the maximum and minimum measurement efficiencies are 97.86% and 95.18%, respectively. The maximum and minimum output powers are divided into 205.93 W and 172.63 W. The fluctuations in efficiency and power are 1.8% and 13.8%, respectively.

From Fig. 9(b), the maximum and minimum measurement efficiencies are 96.06% and 95.07%, respectively, when the offset distance is within 100 mm. The maximum output power is 208.05 W. The fluctuations of transmission efficiency and output power are 0.99% and 3.88%, respectively.

The results show that the fluctuation rate of the transmission efficiency of RSDSC with magnetic cores is very small when the coil is offset. This is because the mutual inductance of RSDSC structure with a magnetic core is also almost constant during the offset.

3.4. Comparative Experiments

In order to further verify the advantages of the structure, the structure of RSDSC is compared with the conventional rectangular coil structure. At the same time, the structure of the RSDSC with the magnetic core is compared with a conventional rectangular structure of coil with the magnetic core. As shown in Table 7, parameters of conventional rectangular coils are demonstrated. The conventional rectangular receiving coil is noted as R_{X5}. Conventional coils have magnetic cores that are sized to just cover the coil. The core position is the same as that of the structure of RSDSC with magnetic cores. To make the comparison experiment more rigorous, the center of the conventional core coil is also skeletonized.

Figures 10(a) and 11(a) show the variation of mutual inductance for a conventional rectangular coil structure and a con-

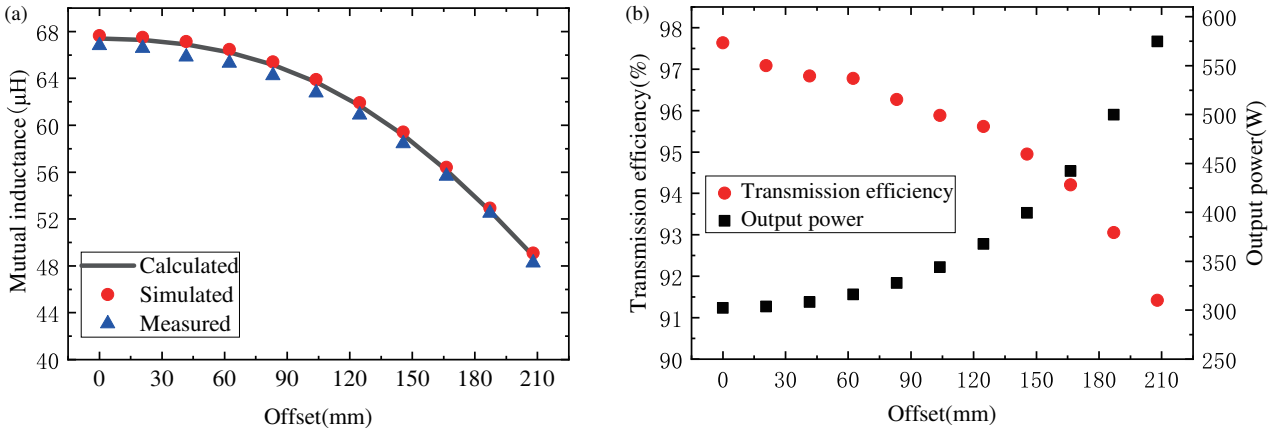

FIGURE 10. Conventional coil structure without magnetic core. (a) Mutual inductance of conventional coil structure. (b) Output power and transmission efficiency of conventional coil structure.

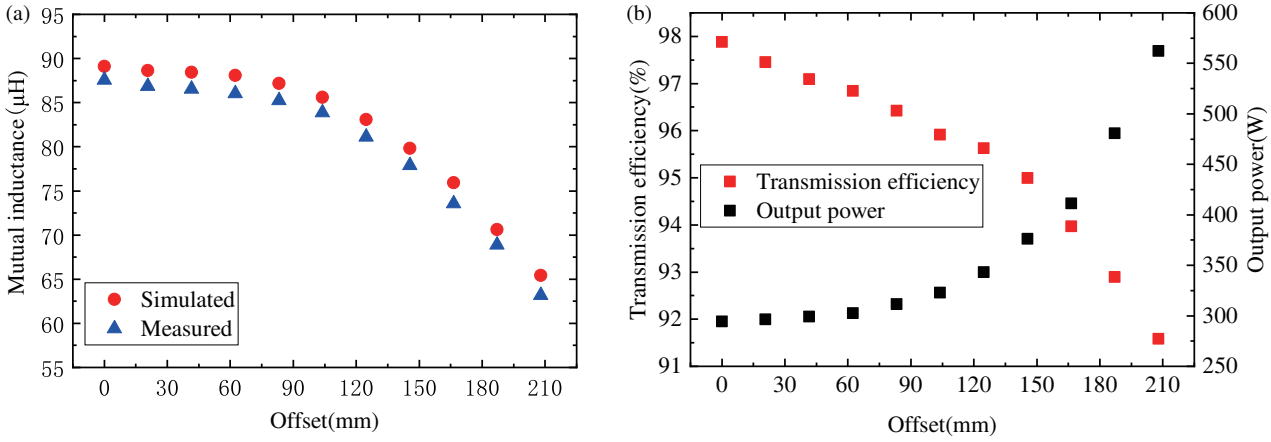

FIGURE 11. Conventional coil structure with magnetic core. (a) Mutual inductance of conventional coil structure with magnetic core. (b) Output power and transfer efficiency of conventional coil structure with magnetic core.

TABLE 7. Experimental parameters of conventional coils.

Coils	Inner length /cm	Inner width /cm	Outside length /cm	Outside width /cm	Turns
T_X	28	28	41.6	41.6	20
R_{X5}	54	54	67.6	67.6	20

ventional coil structure with a magnetic core for offset distances within 20.8 cm along the horizontal direction, respectively. From Fig. 10(a), the mutual inductance decreases from 66.82 μH to 48.25 μH, at which time the mutual inductance fluctuation rate reaches 27.79%. From Fig. 11(a), the mutual inductance decreases from 87.57 μH to 63.19 μH, and the mutual inductance fluctuation rate reaches 27.84%. The mutual inductance is all decreasing.

Figures 10(b) and 11(b) show the trends of the transmission efficiency and output power of conventional coils and conventional coils with magnetic cores when they are offset along the horizontal square, respectively. From Fig. 10(b), the transmission efficiency decreases from 97.13% all the way down to 91.02% when the offset is within 208 mm. Output power increases from 300.86 W to 568.47 W. The fluctuation rate of transmission efficiency and output power is 6.11% and 88.95%, respectively. From Fig. 11(b), the transmission efficiency decreases from 97.88% all the way down to 91.58% at offsets within 208 mm. Output power increased from 294.36 W to 562.24 W. The fluctuation rate of transmission efficiency and output power is categorized as 6.3% and 91.00%.

From the experimental data, the transmission efficiency and output power of the structure of the RSDS coil proposed in this paper and the structure of RSDSC with magnetic core are smaller than the traditional structure. Similarly, it is because the structure of RSDSC has much smaller mutual inductance fluctuation rate than the conventional structure.

4. CONCLUSIONS

In this paper, a symmetric coil structure with a reversed series double layer is proposed. First, the structure of RSDSC is optimally solved according to the parameter optimization method. Further, magnetic core optimization is performed based on the optimal parameters of the coil. The mutual inductance remains essentially unchanged when the receiver coil is offset within 50% of the full length outside the transmitter coil. The experimental results show that the maximum mutual inductance fluctuation changes from 3.77% to 4.88% when the coil horizontal offset distance is within 20.8 cm for the structure of RSDSC with the magnetic core compared to the structure of RSDSC without magnetic core. However, the coupling coefficient increases from 0.1175 to 0.1274, and its maximum efficiency increases from 97.29% to 97.86%. The structure of RSDSC, after magnetic core optimization, is above the standard values set in the industry sector in terms of both system capacity of anti-offset and system transmission efficiency. Therefore, it is very suitable for dynamic wireless charging systems of EV. This paper focuses on the structure of RSDSC and magnetic core optimization based on this structure. However, the structure of RSDSC has strong offset performance only in the direction of EV motion. In the future, the structure needs to be improved so that it can realize stronger anti-offset performance even in the direction of lateral horizontal motion.

ACKNOWLEDGEMENT

This work was supported in part by the National Key Research and Development Program of China under Grant No. 2022YFB3403200, in part by the Natural Science Foundation of Hunan Province under Grant No. 2022JJ30226, and Aid program for Science and Technology Innovative Research Team in Higher Educational Institutions of Hunan Province.

REFERENCES

[1] Wang, Y. J., K. X. Lu, Y. S. Yao, *et al.*, "An electric vehicle (EV)-oriented wireless power transfer system featuring high misalignment tolerance," *Proceedings of the CSEE*, Vol. 39, No. 13, 3907–3917, 2019.

[2] Li, Z., X. Xiong, L. Ren, P. Kong, Y. Zhang, and J. Li, "Design and optimization of quasi-constant coupling coefficients for superimposed dislocation coil structures for dynamic wireless charging of electric vehicles," *Progress In Electromagnetics Research M*, Vol. 116, 23–38, 2023.

[3] Xue, M., Q. Yang, P. Zhang, J. Guo, Y. Li, and X. Zhang, "Application status and key issues of wireless power transmission technology," *Transactions of China Electrotechnical Society*, Vol. 36, No. 8, 1547–1568, 2021.

[4] Su, Y., X. Hou, and X. Dai, "Review of foreign object detection technology in magnetic coupling wireless power transfer system," *Proceedings of the CSEE*, Vol. 42, No. 3, 715–728, 2021.

[5] Shi, L., N. Rasool, H. Zhu, K. Huang, and Y. Yang, "Design and experiment of a reconfigurable magnetic resonance coupling wireless power transmission system," *IEEE Microwave and Wireless Components Letters*, Vol. 30, No. 7, 705–708, 2020.

[6] Chen, Y., B. Yang, Y. Peng, Y. Lu, Z. Zhang, R. Mai, and Z. He, "Review of anti-misalignment technology in inductive wireless power transfer system," *Proceedings of the CSEE*, Vol. 43, 5537–5557, 2023.

[7] Hou, X., Z. Wang, Y. Su, Z. Liu, and Z. Deng, "A dual-frequency dual-load multirelay magnetic coupling wireless power transfer system using shared power channel," *IEEE Transactions on Power Electronics*, Vol. 37, No. 12, 15 717–15 727, 2022.

[8] Liao, Z., Y. Sun, Z. Ye, *et al.*, "Research on resonance mechanism and resonant point distribution characteristic of magnetic coupling wireless power transfer systems," *Transactions of China Electrotechnical Society*, Vol. 35, No. 2, 215–224, 2020.

[9] Wu, L. and B. Zhang, "Overview of static wireless charging technology for electric vehicles: Part II," *Transactions of China Electrotechnical Society*, Vol. 35, No. 08, 1662–1678, 2020.

[10] Zhang, Y., W. Pan, H. Wang, Z. Shen, Y. Wu, J. Dong, and X. Mao, "Misalignment-tolerant dual-transmitter electric vehicle wireless charging system with reconfigurable topologies," *IEEE Transactions on Power Electronics*, Vol. 37, No. 8, 8816–8819, 2022.

[11] Tian, Y., Z. Zhu, L. Xiang, and J. Tian, "Vision-based rapid power control for a dynamic wireless power transfer system of electric vehicles," *IEEE Access*, Vol. 8, 78 764–78 778, 2020.

[12] Chen, J., H. Zhou, Q. Deng, F. Chen, A. Zhu, J. Liu, and X. Gao, "Free-positioning wireless power transfer system based on one-to-multiple topology," *IEEE Transactions on Power Electronics*, Vol. 35, No. 10, 9959–9964, 2020.

[13] Cheng, C., F. Lu, Z. Zhou, W. Li, C. Zhu, H. Zhang, Z. Deng, X. Chen, and C. C. Mi, "Load-independent wireless power transfer system for multiple loads over a long distance," *IEEE Transactions on Power Electronics*, Vol. 34, No. 9, 9279–9288, 2018.

[14] Wu, Y., C. Liu, M. Zhou, X. Mao, and Y. Zhang, "An antioffset electric vehicle wireless charging system based on dual coupled antiparallel coils," *IEEE Transactions on Power Electronics*, Vol. 38, No. 5, 5634–5637, 2023.

[15] Budhia, M., G. Covic, and J. Boys, "A new ipt magnetic coupler for electric vehicle charging systems," in *IECON 2010 — 36th Annual Conference on IEEE Industrial Electronics Society*, 2487–2492, 2010.

[16] Budhia, M., J. T. Boys, G. A. Covic, and C.-Y. Huang, "Development of a single-sided flux magnetic coupler for electric vehicle IPT charging systems," *IEEE Transactions on Industrial Electronics*, Vol. 60, No. 1, 318–328, 2011.

[17] Zaheer, A., G. A. Covic, and D. Kacprzak, "A bipolar pad in a 10-kHz 300-W distributed IPT system for AGV applications," *IEEE Transactions on Industrial Electronics*, Vol. 61, No. 7, 3288–3301, 2013.

[18] Kim, S., G. A. Covic, and J. T. Boys, "Tripolar pad for inductive power transfer systems for EV charging," *IEEE Transactions on Power Electronics*, Vol. 32, No. 7, 5045–5057, 2016.

[19] Li, Z., S. Li, J. Li, *et al.*, "Mutual inductance calculation and optimization of multireceiver positive and negative series coil structure in dynamic wireless power transfer systems," *Transactions of China Electrotechnical Society*, Vol. 36, No. 24, 5153–5164, 2021.

[20] Ahmad, A., M. S. Alam, and A. A. S. Mohamed, "Design and interoperability analysis of quadruple pad structure for electric vehicle wireless charging application," *IEEE Transactions on Transportation Electrification*, Vol. 5, No. 4, 934–945, 2019.

[21] Kong, L. C., H. J. Li, B. Pan, *et al.*, "Research on quadruple D square coil with high misalignment tolerance for wireless power transfer," *Transactions of China Electrotechnical Society*, Vol. 37, No. 13, 3361–3371, 2022.

[22] Wang, Z. H., C. Hu, Y. Sun, *et al.*, "Design of magnetic coupler for inductive power transfer system based on output power and efficiency," *Transactions of China Electrotechnical Society*,

Vol. 30, No. 19, 26–31, 2015.

[23] Chen, Y., R. Mai, Y. Zhang, M. Li, and Z. He, "Improving misalignment tolerance for IPT system using a third-coil," *IEEE Transactions on Power Electronics*, Vol. 34, No. 4, 3009–3013, 2019.

[24] Li, Z. Q., J. Li, C. H. Quan, *et al.*, "Mutual inductance calculation of arbitrarily positioned rectangular coils with magnetic shielding in wireless power transfer systems," *Transactions of China Electrotechnical Society*, Vol. 37, No. 17, 4294–4305, 2022.